CHIN. PHYS. LETT. Vol. 34, No. 11 (2017) 118102

Fabrication and Characterization of a GaN-Based 320×256 Micro-LED Array *

Xiao-Fan Mo(莫晓帆), Wei-Zong Xu(徐尉宗), Hai Lu(陆海)**, Dong Zhou(周东), Fang-Fang Ren(任芳芳), Dun-Jun Chen(陈敦军), Rong Zhang(张荣), You-Dou Zheng(郑有炓)

Jiangsu Provincial Key Laboratory of Advanced Photonic and Electronic Materials, and School of Electronic Science and Engineering, Nanjing University, Nanjing 210093

(Received 22 May 2017)

Design, fabrication and characterizations of GaN-based blue micro light emitting diode (LED) arrays are reported. The GaN micro-LED array consists of 320 × 256 pixels with a pitch size of 30 μm. Each pixel is 25 × 25 μm² in size, which is designed for backside emission and high density flip-chip packaging. The selected LED pixels being tested exhibit good uniformity in terms of turn-on voltage and reverse leakage current. The efficiency droop behavior and reliability behavior under high forward current stress are also studied. The micro-LED pixel shows improved reliability, which is likely caused by enhanced heat dissipation.

PACS: 81.05.Ea, 85.60.Jb, 72.10.Bg DOI: 10.1088/0256-307X/34/11/118102

Compared with conventional light emitting diodes (LEDs), which are currently being massively used in various solid-state lighting and liquid crystal display (LCD) back-lighting areas, micro-LEDs have recently emerged as a new type of light emitting devices, which have received world-wide interest. Due to their unique characteristics of high modulation speed and fast programmable emission pattern, micro-LED arrays have been demonstrated in a variety of novel applications, such as visible light communication (VLC), direct LED writing, optogenetics, implantable vision aid and micro-LED displays.[1,2] Among these applications, micro-LED displays are very attractive as they are particularly suitable for virtual reality display areas, which have a fast growing market.[3] Compared with the widespread LCD technology, micro-LED displays offer far greater contrast, much faster response time, and would consume less energy.

However, compared with the mature LED fabrication technology, micro-LED displays are still in their early development stage. There is still no commonly-accepted cost-effective fabrication technology for realizing full-color micro-LED displays. There is also intense competition between organic micro-LED and inorganic micro-LED approaches.[4,5] Although inorganic micro-LEDs, especially GaN-based micro-LEDs, should theoretically have much higher output power and better reliability, the related experimental study is still quite limited until recently, while high current operation is required in some applications like VLC and organic laser pumping.[6]

In this work, a GaN-based 320×256 micro-LED array is designed and fabricated. The micro-LEDs sharing a common cathode are individually addressable, which are ready to be flip-chip packaged with the silicon driver circuit. Similar efficiency droop behavior of the micro-LED pixel is observed compared with that of conventional large area devices. The reliability characteristics of the micro-LED pixel stressed at very high forward current density is also studied.

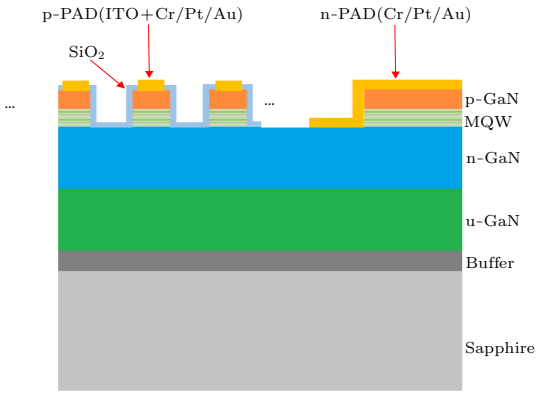


Fig. 1. Cross-sectional schematic diagram of the fabricated micro-LED structure.

As shown in Fig. 1, the micro-LED arrays are fabricated on a standard GaN blue LED epi-wafer. The epi-structure is grown on a 2-inch sapphire substrate by using metal-organic chemical vapor deposition, which consists of a 2.5 μm undoped GaN buffer layer, a 3.2 μm GaN:Si n-contact layer, a 10 period InGaN/GaN (2 nm/8 nm), multi-quantum wells (MQWs), an AlGaN electron blocking layer, and a 270 nm GaN:Mg p-contact layer. The micro-LED pixels are fabricated through a similar process for flip-chip LEDs, which starts with mesa etching. An evaporated ITO layer is then deposited for the p ohmic contact, which is patterned and annealed in N_2 atmosphere for 1 min at 600℃. Next, the devices are passivated by a 500 nm SiO_2 layer deposited by plasma enhanced chemical vapor deposition, which is followed by contact window opening by wet chemical etching. Finally, thick metal stacks based on Cr/Pt/Au trilayer are used for the n ohmic contact as well as the contact pads for both p and n electrodes.

*Supported by the National Key Research and Development Program under Grant No 2016YFB0400902, and the Science and Technology Project of State Grid Corporation of China under Grant No SGSDDK00KJJS1600071.

**Corresponding author. Email: hailu@nju.edu.cn

© 2017 Chinese Physical Society and IOP Publishing Ltd

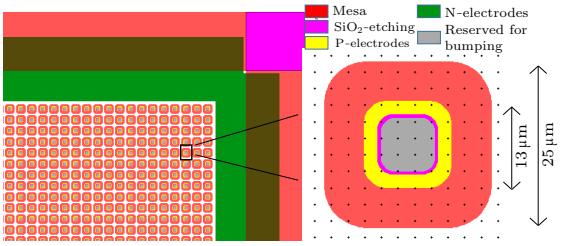


Fig. 2. Snapshot layout image of the fabricated micro-LED arrays.

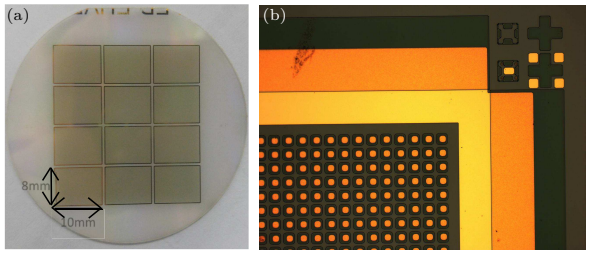


Fig. 3. (a) Top-view image of the fabricated micro-LED arrays on 2-inch sapphire wafer. (b) Microscopic image of the fabricated micro-LED array.

The detailed layout information of the GaN micro-LED array is shown in Fig. 2. Each array consists of 320×256 pixels arrayed in orthogonal configuration. The pitch length between adjacent pixels is 30 μm while the mesa size of each pixel is 25 μm. All pixels have independent p-contacts, which are ready for connecting with the silicon driver circuit by using indium bumps. A large size cathode electrode is made outside the array area, which is shared by all LED pixels. In future flip-chip packaging processes, multiple indium bumps will be made on the cathode electrode surrounding the array area to ensure efficient and uniform current injection. Figure 3 shows the top-view image of one processed 2-inch epi-wafer as well as the microscopic image of the micro-LED array. The whole 320×256 micro-LED array is about $8 \times 10\,\mathrm{mm}^2$ in size. As a result, up to 12 micro-LED arrays can be fabricated on a single 2-inch sapphire wafer.

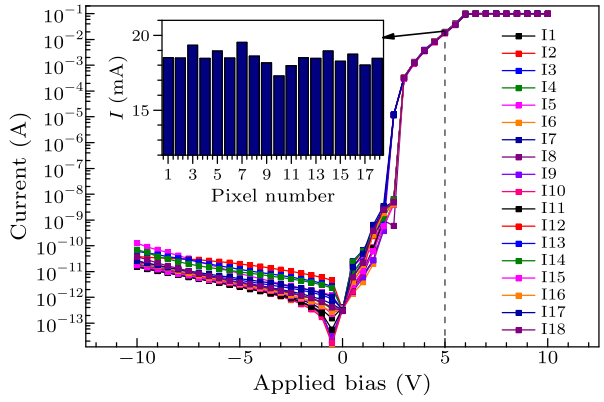


Fig. 4. The typical I–V characteristics of the fabricated micro-LED pixels. Inset: forward current at 5 V of 18 randomly selected pixels.

Current-voltage (I–V) characterizations of the micro-LED pixels are firstly conducted. Since there are over 80000+ pixels in each array and the pixel size is only 20–30 μm, even the I–V curve mapping by automatic prober would be difficult. As a result, 18 representative pixels are randomly selected from the micro-LED array for I–V testing. As shown in Fig. 4, these 18 micro-LEDs show fairly consistent I–V characteristics with on/off ratio over 10^9 (±5 V). The reverse leakage current of these LEDs are all below 0.1 nA at −5 V bias. The forward I–V characterizes can be fitted by the standard p–n diode equation

$$I = I_0(e^{qV_\mathrm{f}/nKT} - 1),$$

where I is the forward current, I_0 is the reverse saturation current, V_f is the forward bias, K is the Boltzmann constant, and n is the ideality factor. The ideality factor n is extracted from the I–V curves using the standard procedure in Ref. [7], which is shown in Fig. 5 as a function of the forward current density.

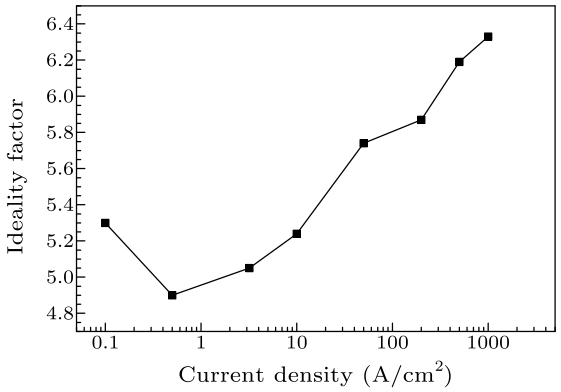


Fig. 5. The extracted ideality factor n of the micro-LED as a function of the forward current density.

For p–n junction diodes, normally ideality factors between 1.0 and 2.0 are attributed to the competition between the carrier drift diffusion process and the Sah–Noyce–Shockley generation recombination process. A high n obtained at low forward bias could be caused by trap-assisted tunneling related leakage. As shown in Fig. 5, at low current density (<1 A/cm^2), the ideality factor of the micro-LED firstly decreases as the injection current density increases, which means that the diffusion current still accounts for a considerable part at this current density level. When the injection current density further increases (>1 A/cm^2), the ideality factor starts to continuously increase, which should be caused by enhanced tunneling current. In this work, the calculated n would reach 6.7–7.0. Similar high ideality factors have been reported in conventional large-area GaN-based LEDs,[8] which is likely caused by polarization-induced triangular band profiles of the quantum barriers within the LED structure. These micro-LEDs also have good uniformity in terms of turn-on voltage and series resistance. As shown in the inset of Fig. 4, at a fixed forward bias of 5 V, the forward currents of these devices vary slightly from 18.25 to 19.43 mA.

The light emitting performance of the micro-LED pixels at different current injection levels is further studied. Figure 6(a) shows the normalized external quantum efficiency (EQE) of a micro-LED as a function of the injection current density. A typical efficiency droop behavior is observed, in which the maximum EQE occurs at $\sim$3 A/cm^2 and then gradually drops at higher injection current density. The efficiency droop behaviors of the micro-LED and the large size LEDs fabricated on the same epi-wafer are compared in Fig. 6(b). It is clear that the peak efficiency currents of these LEDs are almost the same, while at higher current density (>10 A/cm^2), the EQE of the micro-LED pixel drops more slowly than its larger sized counterparts. The efficiency droop effect widely observed in GaN-based LEDs is caused by a non-radiative carrier loss mechanism that becomes dominant as the injection current increases. Until recently, there was no agreement on the exact physical mechanism for this effect. Electron leakage,[9] lack of hole injection,[10,11] carrier delocalization,[12,13] Auger recombination, defects,[14] and junction heating have been suggested as possible explanations. Smaller chip size could certainly benefit current spreading and heat dissipation. Greater strain relaxation within the MQWs is also possible for micro-LEDs which have a larger height-to-width aspect ratio. Nevertheless, if effects, like Auger recombination, are the dominant mechanism for efficiency droop, micro-LEDs should suffer from similar efficiency degradation at high injection current compared with that of large area GaN-based LEDs.

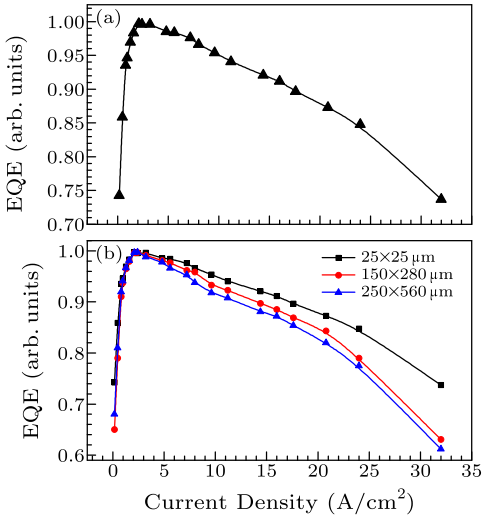


Fig. 6. (a) Normalized external quantum efficiency of a micro-LED pixel as a function of the injection current density. (b) Comparison of droop behaviors between the micro-LED pixel and LED chips with larger size.

Finally, the aging behavior of the GaN micro-LEDs operating at high injection current level is preliminarily studied. Since for many potential applications it is preferable for micro-LEDs to be driven at high current to achieve high light output power and high modulation bandwidth, in this work the micro-LED chip is stressed at a very high forward current density of 3.2 kA/cm^2 to accelerate its performance degradation. A direct impact of high current stress to the unpackaged LED chip is the high junction temperature. Figure 7 shows the measured light output power ($P_{\rm out}$) of a stressed micro-LED as a function of stress time. It is found that within the first 20 h, $P_{\rm out}$ of the micro-LED shows a slight increase up to $\sim$12% instead of a consistent drop. A similar effect has been reported for large-area GaN-based LEDs under aging test, which is caused by the improved current spreading property of the p-GaN contact layer. It has been reported that under a combined effect of high junction temperature and high current flow, the p-type conductivity of Ga:Mg can be more effectively activated. Amano *et al.* firstly realized p-type conductivity in GaN:Mg based on a post-growth low-energy electron beam irradiation treatment, which was later found to be effective even at the liquid-helium temperature.[15,16] Thus the forward current stress may act as a minority-carrier injection process, which also helps to activate Mg dopants. After the initial $P_{\rm out}$ rise and then an intermediate platform region, $P_{\rm out}$ starts to drop slowly. Since $P_{\rm out}$ drops at a nearly constant rate as a function of stress time, based on linear fitting and extrapolation, the estimated lifetime (at 90% $P_{\rm out}$) of the micro-LED chip is $\sim$156 h under high current stress. Although the lifetime estimated here is much less than that of commercial GaN-based LEDs, considering the extremely high stress current of 3.2 kA/cm^2 used in the aging test, the micro-LED fabricated in this work still shows promising reliability. In addition, here it should be noted that the micro-LED chip under test is unpackaged with a partly fulfilled heat dissipation capability. Improved reliability and lifetime are expected after the micro-LED array is flip-chipped with indium bumps.

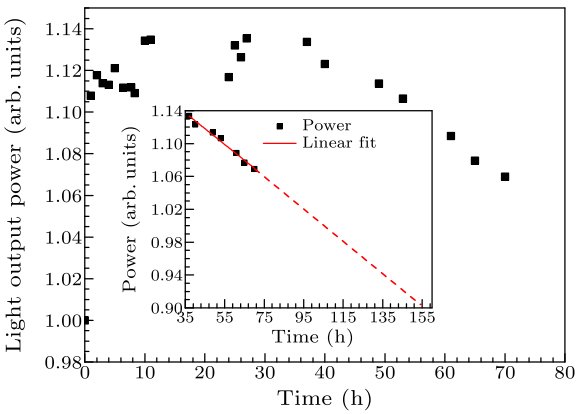


Fig. 7. Normalized light output power of a micro-LED pixel versus stress time. Inset: linear fit of the micro-LED's aging characteristics.

The aging test is conducted under a forward current density of 3.2 kA/cm^2 at room temperature. During the aging test, I–V characteristics are measured

periodically for understanding the performance degradation behavior. Figure 8(a) shows the I–V curves of the micro-LED before and after the tests of 17 and 40 h. It is clear that both the reverse leakage current and low-forward-bias leakage current would increase upon the high current stress, which should be related to new defects generated within the LED junction. Based on past reliability studies, these new induced defect are mostly non-radiative recombination centers, which would reduce the internal quantum efficiency (IQE) of the micro-LED and would lead to a slight rise of the ideality factor n as shown in Fig. 8(c). That is, in spite of the observed initial rise of light output in Fig. 6, generation of defects happens in a progressive way and the IQE of the micro-LED would drop upon high current stress. Figure 8(b) shows $P_{\rm out}$ versus injection current density curves measured after the micro-LED is stressed for 17 and 40 h, respectively. It is clear that the $P_{\rm out}$ degradation occurs in the entire injection current range instead of a high current phenomenon only, which confirms the IQE reduction. Thus the I–V and $P_{\rm out}$–I characterization again suggest that the initial rise of light output is caused by enhanced current spreading and hole supply, which are outperformed by the IQE degradation at prolonged high current stress time.

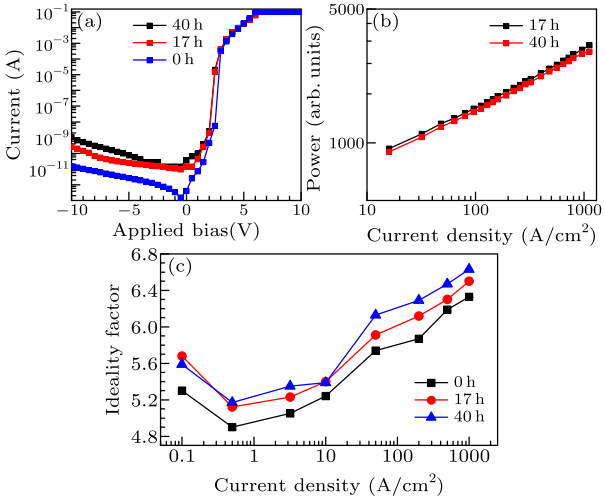


Fig. 8. The variation of I–V curves (a), output power versus injection current density (b), and the ideality factor n (c) of the micro-LED pixel after the stresses of 17 and 40 h.

In summary, a 320 × 256 GaN-based micro-LED array has been designed and fabricated. The micro-LEDs within the array have a pixel size of $25 \times 25\,\mu{\rm m}^2$ and share a common cathode, which are ready to be flip-chip packaged with the Si driver circuit. The efficiency droop characteristics of the micro-LED pixel are studied, which shows slightly reduced droop behavior compared with that of large-size GaN-based LEDs. When the micro-LED pixel is stressed by very high current, the micro-LED exhibits three-stage degradation behavior, including an initial improvement stage, a platform stage, and then a consistent degradation stage. The initial $P_{\rm out}$ rise is likely caused by the improvement of p-GaN conductivity induced by thermo- and high current co-stressing, which is later counterbalanced and surpassed by new defect related IQE degradation.

References

[1] McKendry J J D, Massoubre D, Zhang S, Rae B R, Green R P, Gu E, Henderson R K, Kelly A E and Dawson M D 2012 *J. Lightwave Technol.* **30** 61
[2] Li X, Bamiedakis N, Wei J L, McKendry J J D, Xie E, Ferreira R, Gu E, Dawson M D, Penty R V and White I H 2015 *J. Lightwave Technol.* **33** 3571
[3] Zhang H X, Massoubre D, McKendry J, Gong Z, Guilhabert B, Griffin C, Gu E, Jessop P E, Girkin J M and Dawson M D 2008 *Opt. Express* **16** 9918
[4] Hahn B, Galler B and Engl K 2014 *Jpn. J. Appl. Phys.* **53** 100208
[5] Meneghini M, Tazzoli A, Meneghesso G and Zanoni E 2010 *IEEE Trans. Electron Devices* **57** 108
[6] Meneghini M, Lago M D, Trivellin N, Meneghesso G and Zanoni E 2014 *IEEE Trans. Ind. Appl.* **50** 78
[7] Shah J M, Li Y L, Gessmann T H and Schubert E F 2003 *J. Appl. Phys.* **94** 2627
[8] Lu T P, Li S T, Zhang K, Liu C, Xiao G W, Zhou Y G, Zheng S W, Yin Y A, Wu L J, Wang H L and Yang X D 2011 *Chin. Phys.* B **20** 098503
[9] Lin R M, Yu S F, Chang S J, Chiang T H, Chang S P and Chen C H 2012 *Appl. Phys. Lett.* **101** 081120
[10] Pope I A, Smowton P M, Blood P, Thomson J D, Kappers M J and Humphreys C J 2003 *Appl. Phys. Lett.* **82** 2755
[11] Xie J, Ni X, Fan Q, Shimada R, Ozgur U and Morkoc H 2008 *Appl. Phys. Lett.* **93** 121107
[12] Kim A Y, Gotz W, Steigerwald D A, Wierer J J, Gardner N F, Sun J, Stockman S A, Martin P S, Krames M R, Kern R S and Steranka F M 2001 *Phys. Status Solidi* A **188** 15
[13] Chichibu S F, Azuhata T, Sugiyama M, Kitamura T, Washida Y, Okumurac H, Nakanwashi H, Sota T and Mukai T 2001 *J. Vac. Sci. Technol.* B **19** 2177
[14] Shen Y C, Muller G O, Watanabe S, Gardner N F, Munkholm A and Krames M R 2007 *Appl. Phys. Lett.* **91** 141101
[15] Jiang R, Lu H, Chen D J, Ren F F, Zhang R and Zheng Y D 2013 *Chin. Phys.* B **22** 047805
[16] Tian P F, Althumali A, Gu E D, Watson I M, Dawson D M and Semicond R 2016 *Semicond. Sci. Technol.* **31** 045005